Convolution-Based Data-Driven Simulation and Controller Design Method

Naoki Kameya, Yasutaka Fujimoto, *Senior Member, IEEE*, Yu Hosoyamada, *Member, IEEE*, and Toyoaki Suenaga

***Abstract*—Some of the challenges in data-driven control are the selection of the nominal model of the closed-loop system that gives the fastest response achievable and the validation of the tuning results. The virtual time-response-based iterative gain evaluation and redesign (V-Tiger) method is an approach to solve the problems in data-driven control, but it cannot account for the nonlinearity of the controller. The article proposes a data-driven simulation and controller design approach named the convolution-based data-driven simulation (CDDS) method. Based on time-domain convolution operations, the method enables closed-loop simulations without building a plant model. The method offers various approaches for controller design, such as directly specifying the overshoot and settling time and achieving the desired characteristics. Unlike the conventional methods, the CDDS method can explicitly handle the nonlinearity of the controller and is expected to be applicable to a wide range of control systems. The results of experiments conducted using a buck converter indicate that the CDDS method can reduce the estimation error by up to 95.0% compared with the conventional V-Tiger method. Furthermore, it can reduce the tuning error by more than 52.0% compared with the virtual reference feedback tuning and noniterative correlation-based tuning methods.**

***Index Terms*—Control system synthesis, dc–dc power converters, digital control, simulation, voltage control.**

I. Introduction

DATA-DRIVEN control approaches have recently attracted increasing attention, and numerous practical methods were proposed for a range of industrial control applications [1], [2], [3], [4], [5], [6], [7], [8], [9], [10], [11]. Recent trends in data-driven control have been reported in [1]. In particular, reinforcement learning and other learning-based methods have been comprehensively studied. Many applications have been proposed for tuning proportional–integral–derivative controllers [12], [13], [14], [15], [16], which are the main type of closed-loop controller [17]. Some of them have reported that the response was significantly improved by introducing data-driven control compared with conventional model-based methods in practice [16]. Such a data-driven control approach eliminates the need to construct a plant model and also enables a control design that takes into account various behaviors of the entire system, which are often difficult to consider directly. For example, virtual reference feedback tuning (VRFT) method requires only one set of input and output data for the plant to tune its control parameters [4]. The VRFT method can, therefore, be used in the mass production of products that require controller tuning to account for the variations in the system characteristics. However, information on the plant and tuning of the nominal model through multiple experiments is necessary to achieve the fastest feasible response by this method because it requires a nominal model, and the optimal nominal model depends on the constraints of the physical responses of the plant. Furthermore, it is desirable to know the response of the parameters obtained via the VRFT method in advance to assess system safety. Other conventional control methods, such as the fictitious reference feedback tuning [5] and noniterative correlation-based tuning (NCbT) [6] methods, have similar plant and/or nominal model requirements. Several learning-based data-driven control approaches have also been proposed [7], [8], [9], [10], [11], but these approaches are computationally intensive and often require large amounts of experimental data.

Data-driven simulation has been proposed as an alternative to data-driven control approaches [18], [19], [20], [21], [22]. In data-driven simulation, the plant response is estimated when the input and output data of the plant and the desired control inputs are given. For this estimation, a subspace method is often integrated to effectively create a model-free method that avoids the inherent complexities of conventional control methods [18], [19]. Since a state-space model framework is considered, these subspace-method-based approaches work well with feedback-based controller design methods, such as the linear quadratic regulator. However, there are inherent difficulties when applying these approaches to controllers that process nonlinearity because the control input must be provided in advance. Furthermore, nonlinearities often appear in the control inputs. For example, if the controller output, namely, the control input, has a saturation characteristic, then it is necessary to sequentially check whether

Manuscript received 31 March 2023; revised 13 August 2023; accepted 27 September 2023. *(Corresponding author: Naoki Kameya.)*

Naoki Kameya and Yasutaka Fujimoto are with the Department of Electrical and Computer Engineering, Yokohama National University, Yokohama 240-8501, Japan (e-mail: kameya-naoki-ms@ynu.jp; fujimoto@ynu.ac.jp).

Yu Hosoyamada is with the R&D Center, Kyosan Electric Manufacturing Company Ltd., Yokohama 230-0031, Japan (e-mail: yu-hosoyamada@kyosan.co.jp).

Toyoaki Suenaga is with the Department of Power Electronics Division, Kyosan Electric Manufacturing Company Ltd., Yokohama 230-0031, Japan (e-mail: to-suenaga@kyosan.co.jp).

Color versions of one or more figures in this article are available at https://doi.org/10.1109/TIE.2023.3323746.

Digital Object Identifier 10.1109/TIE.2023.3323746

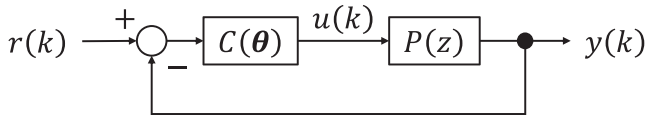

Fig. 1. Assumed discrete-time feedback system. $P(z)$, $C(\boldsymbol{\theta})$, $r(k)$, $u(k)$, and $y(k)$ are the plant, controller parameterized by $\boldsymbol{\theta}$, reference value, control input, and plant output, respectively.

the control input saturates to account for this characteristic. Therefore, the output data from the plant are required to perform this check. Similarly, several of the proposed approaches that are not based on the state-space model assume a linear system, and hence, they cannot take into account the system nonlinearities [20], [21], [22].

This work proposes a new controller design method based on a new data-driven simulation method. This new method is called the convolution-based data-driven simulation (CDDS) method. The motivation for introducing CDDS is to deal with the nonlinearities that cannot be handled in the conventional data-driven simulations described so far. The proposed CDDS method is then applied to controller design with three types of optimization approaches investigated: direct optimization using a specified evaluation criterion, iterative optimization using gradient information, and optimization via a single calculation. While there are notable differences in the computational costs of the three approaches, these methods share the common feature that a controller is designed without building a plant model. The main contributions of this work can be summarized in two points. One is that CDDS provides a data-driven simulation method for controllers with nonlinearities, and the other one is that CDDS provides a data-driven controller design method that explicitly accounts for controller nonlinearities.

The rest of this article is organized as follows. The basic theory and algorithms of the CDDS are explained in Section II, and the CDDS-based controller design method is described in Section III. The CDDS method is then applied to the controller design of a buck converter and compared with the conventional control method results in Section IV. Finally, Section V concludes this article.

II. Convolution-based Data-Driven Simulation

Here, the CDDS method, a type of data-driven simulation method is proposed. The basic theory of CDDS is first explained and then generalized.

A. Problem Settings

A discrete-time feedback system is assumed with a block diagram of the system shown in Fig. 1. Further, $P(z)$, $C(\boldsymbol{\theta})$, $r(k)$, $u(k)$, and $y(k)$ represent the plant, controller (parameterized by $\boldsymbol{\theta}$), reference value, control input, and plant output, respectively. Here, k represents a given time sample and takes an integer value such that $k \geq 0$ is assumed. The plant model $P(z)$ is used for convenience in the future discussions. However, note that $P(z)$ will not appear explicitly in the final results.

B. Basic Theory of CDDS

Several assumptions were made about the plant and experimental data when considering the proposed CDDS method.

The first assumption is that the plant can be assumed as a linear time-invariant (LTI) system. Importantly, note that there are no restrictions on the controller, such that the controller can be either linear or nonlinear. The following equations hold in the z-domain as the plant is an LTI system:

$$Y_0(z) = P(z)U_0(z) \tag{1}$$

and

$$Y(z) = P(z)U(z) \tag{2}$$

where $U_0(z)$ and $Y_0(z)$ are the experimental input and output data in the z-domain, respectively, and $U(z)$ and $Y(z)$ are the simulated input and output data in the z-domain, respectively. $Y(z)$ is the only unknown in this system of equations as $U(z)$ is given at the time of the simulation. The following relationship between (1) and (2) can be obtained by canceling $P(z)$:

$$Y(z)U_0(z) = U(z)Y_0(z). \tag{3}$$

Two new assumptions were introduced to obtain the time-domain signal of the estimated output $Y(z)$. One assumption is that the state of the plant prior to the zeroth sample in the experimental data is negligible. This assumption ensures causality in the experimental data. Therefore, the responses that start from either the zero state or some constant value that is sufficiently convergent are available as experimental data. The second assumption is that the first input datum $u_0(0)$ in the experimental data is a nonzero value. The reason for this assumption will become clear when (3) is transformed into a time-domain signal. A convolution operation is performed on each side of (3) for transformation into a time-domain signal. This operation yields the following relationship:

$$y(k) * u_0(k) = u(k) * y_0(k). \tag{4}$$

That is

$$\sum_{i=0}^{k} y(i)u_0\left(k-i\right) = \sum_{i=0}^{k} u(i)y_0\left(k-i\right). \tag{5}$$

The signal for the kth time sample can be separated to obtain

$$\begin{aligned} &y(k)u_0(0) + \sum_{i=0}^{k-1} y(i)u_0\left(k-i\right) \\ &= u(k)y_0(0) + \sum_{i=0}^{k-1} u(i)y_0\left(k-i\right). \end{aligned} \tag{6}$$

Then, assumptions of $y_0(0) = 0$ and $u_0(0) \neq 0$ are applied to calculate the output for the kth time sample $y(k)$ using the data up to the $(k-1)$th time sample

$$y(k) = \frac{1}{u_0(0)}\left(\sum_{i=0}^{k-1} u(i)y_0\left(k-i\right) - \sum_{i=0}^{k-1} y(i)u_0\left(k-i\right)\right). \tag{7}$$

Note that from (5), $y(0) = 0$. Even if $y_0(0) = 0$ is not satisfied, the calculation can still be performed by canceling $y_0(0)$ as an offset, if the state of the plant is sufficiently convergent at the start of the experiment. This process is described in the next section as a generalization of CDDS.

C. Generalization of CDDS

This study considers the relaxation of the condition on the initial state of the experimental data for the presented CDDS method. A steady state is assumed for the plant at the time of data collection. The input and output data converge at u_{offset} and y_{offset}, respectively. The input and output data obtained in this situation ensure causality, however, they often do not satisfy the conditions during the initial state of the plant. Therefore, the following signals, with their associated offsets removed, are prepared:

$$\bar{u}_0(k) = u_0(k) - u_{\text{offset}} \tag{8}$$

$$\bar{y}_0(k) = y_0(k) - y_{\text{offset}}. \tag{9}$$

These modified input $\bar{u}_0(k)$ and output $\bar{y}_0(k)$ data now satisfy all of the conditions for CDDS, thereby allowing the execution of CDDS. By substituting the modified input $\bar{u}_0(k)$ and output $\bar{y}_0(k)$ data into the CDDS in (7), we can derive the general input and output data as follows:

$$y(k) = \frac{1}{\bar{u}_0(0)} \left(\sum_{i=0}^{k-1} u(i)\bar{y}_0\left(k-i\right) - \sum_{i=0}^{k-1} y(i)\bar{u}_0\left(k-i\right) \right). \tag{10}$$

D. Long-Term Simulation With CDDS

The CDDS formula in (10) indicates the equality of the result obtained by the convolution operations between the estimated input $u(k)$ and output data $\bar{y}_0(k)$, and that obtained by the convolution operations between the estimated output $y(k)$ and input data $\bar{u}_0(k)$. This means that if the experimental data can be obtained, such that $\bar{u}_0(l) = u_{\text{offset}}$ and $\bar{y}_0(l) = y_{\text{offset}}$ for $l \geq N-1$, then it is possible to run a long-term simulation regardless of the number of experimental data samples N. Therefore, the CDDS equation for $k > N-1$ in this case

$$y(k) = \frac{1}{\bar{u}_0(0)} \left(\sum_{i=1}^{N-1} u\left(k-i\right)\bar{y}_0(i) - \sum_{i=1}^{N-1} y\left(k-i\right)\bar{u}_0(i) \right). \tag{11}$$

E. Consideration of Noisy Data and Convergence

When applying CDDS to actual systems, it is necessary to consider the noise in the experimental data. Here, the modified versions of (1) and (2) with noise as the observed noise can be treated as follows:

$$Y_0(z) = P(z)U_0(z) + N_0(z) \tag{12}$$

$$Y(z) = P(z)U(z) + E(z) \tag{13}$$

where $N_0(z)$ is the observed noise in the experimental data, and $E(z)$ is the estimation error of the CDDS. Calculating the same relationship equation as in (3) yields

$$\left(Y(z) - E(z)\right)U_0(z) = U(z)\left(Y_0(z) - N_0(z)\right). \tag{14}$$

Using (3) and (14), we get

$$\begin{aligned} E(z)U_0(z) &= \left(Y(z) - \left(Y(z) - E(z)\right)\right)U_0(z) \\ &= Y(z)U_0(z) - U(z)\left(Y_0(z) - N_0(z)\right) \\ &= U(z)N_0(z). \end{aligned} \tag{15}$$

Therefore, the estimation error $E(z)$ of the CDDS is affected only by the noise observed in the experimental data $N_0(z)$ and the input data $U_0(z)$ and $U(z)$. Assuming that the conditions for the long-term simulation of CDDS hold, the state equation of the time-domain signal for the estimation error $e(k)$ from (11) is set as follows:

$$\begin{aligned} \boldsymbol{e}\left(k+1\right) &= \begin{bmatrix} 0 & 1 & \cdots & 0 \\ 0 & 0 & \cdots & 0 \\ \vdots & \vdots & \ddots & \vdots \\ 0 & 0 & \cdots & 1 \\ -\frac{u_0(N-1)}{u_0(0)} & -\frac{u_0(N-2)}{u_0(0)} & \cdots & -\frac{u_0(1)}{u_0(0)} \end{bmatrix} \boldsymbol{e}(k) \\ &\quad + \begin{bmatrix} 0 & 0 & \cdots & 0 \\ 0 & 0 & \cdots & 0 \\ \vdots & \vdots & \ddots & \vdots \\ \frac{y_0(N-1)}{u_0(0)} & \frac{y_0(N-2)}{u_0(0)} & \cdots & \frac{y_0(1)}{u_0(0)} \end{bmatrix} \boldsymbol{u}(k) \\ &:= \boldsymbol{A}\boldsymbol{e}(k) + \boldsymbol{B}\boldsymbol{u}(k) \end{aligned} \tag{16}$$

where $\boldsymbol{e}(k) = [e(k-(N-1)) \quad \cdots \quad e(k-1)]^T$ and $\boldsymbol{u}(k) = [u(k-(N-1)) \quad \cdots \quad u(k-1)]^T$. Finally, the convergence of the estimation error of the CDDS can be determined by the eigenvalues of matrix $\boldsymbol{A}$ in (16); that is, convergence is achieved if the eigenvalues are inside the unit circle.

F. CDDS Algorithm

Both, the system to be simulated and the experimental conditions must satisfy the assumptions made in the previous section, namely:

1) The system is an LTI system.
2) The output before the zeroth sample [i.e., before time zero ($k < 0$)] in the experiment can be ignored.
3) The initial input $\bar{u}_0(0)$ is nonzero.

These assumptions must be satisfied to ensure that (10) yields valid experimental data, whereby the output of the kth time sample can be computed from the known data up to the $(k-1)$th time sample. Therefore, the output $y(k)$ of the system for any input $u(k)$ can be simulated without any model by adopting the following approach:

1) Collect input $\bar{u}_0(k)$ and output $\bar{y}_0(k)$ data for the system to be simulated; these data are collected through experiments.
2) Calculate the first input $u(0)$ in the simulation.
3) Calculate the output $y(k)$ of the kth time sample from (10).

Theoretically, CDDS can be performed even if the plant is unstable, but in practical use, a stabilizing controller should be

used to obtain experimental data. In addition, the number of experimental data samples N should be large enough to reproduce the response to be simulated. For example, the response of a second-order system converges to 0.0125% of the steady state in three times the 5% settling time. Therefore, N should be at least three times the number of samples for the 5% settling time.

III. CDDS-Based Controller Design Methods

A. Condition Settings

The controller can be designed using the data-driven simulation presented in the previous section. Unlike the plant constraints considered in the simulation, the condition imposed on the controller is simple: the control input of the controller is uniquely determined for a given input. The simple feedback system shown in Fig. 1 is assumed to be a controller that satisfies this condition.

B. Direct Optimization Approach

Direct optimization via the CDDS method is possible when an evaluation function for the plant response is devised. Toward this end, the control parameters are provided as inputs to an optimization solver, such as a metaheuristic algorithm, and this solver helps determine the control parameters that either minimize or maximize the specified evaluation function.

Therefore, an evaluation function $J_{\mathrm{DO}}(\boldsymbol{\theta})$ should be designed to realize this CDDS-based direct optimization approach. For example, $J_{\mathrm{DO}}(\boldsymbol{\theta})$ can take the form of a function that minimizes the 2-norm of a desired reference value $r(k)$ and the output value $y(k)$

$$\begin{aligned} J_{\mathrm{DO}}(\boldsymbol{\theta}) &:= \|r(k) - y(k;\boldsymbol{\theta})\|_2^2 \\ &= \frac{1}{N}\sum_{k=0}^{N-1}\left(r(k) - y(k;\boldsymbol{\theta})\right)^2 \end{aligned} \tag{17}$$

and the optimal parameter vector of the controller $\boldsymbol{\theta}^*$ is

$$\begin{aligned} \boldsymbol{\theta}^* &= \arg\min_{\boldsymbol{\theta}} J_{\mathrm{DO}}(\boldsymbol{\theta}) \\ &= \arg\min_{\boldsymbol{\theta}} = \frac{1}{N}\sum_{k=0}^{N-1}\left(r(k) - y(k;\boldsymbol{\theta})\right)^2. \end{aligned} \tag{18}$$

Note that (18) can be easily solved using a heuristic algorithm, such as the Nelder–Mead method [23]. The obtained parameter vector of the controller $\boldsymbol{\theta}$ can then be used in the CDDS to evaluate the feasibility of achieving the desired performance.

C. Iterative Approach

Using a heuristic algorithm to solve (18) is often a computationally intensive approach. However, if the evaluation function is differentiable by the parameter vector of the controller $\boldsymbol{\theta}$, then a gradient method, such as Newton's method can be used to solve (18) in a more computationally efficient manner.

Let us consider the model reference approach, shown in Fig. 2, as an example. Let $M(z)$ be the nominal model of the desired characteristic of the closed-loop system. The desired output

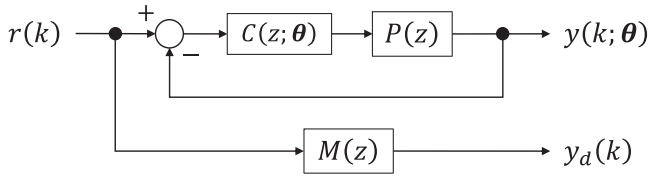

Fig. 2. Model reference control problem. $M(z)$ and $y_d(k)$ are the nominal model and desired output signal, respectively.

$y_d(k)$ for a given reference value $r(k)$ is then given as

$$y_d(k) = M(z)r(k). \tag{19}$$

Furthermore, the controller is assumed to be linearly separable into its associated parameter vector of the controller as follows:

$$C(z;\boldsymbol{\theta}) = \boldsymbol{C}_0^T(z)\boldsymbol{\theta}. \tag{20}$$

The CDDS-based evaluation function is then written as

$$\begin{aligned} J_{MR}(\boldsymbol{\theta}) &:= \|y_d(k) - y(k;\boldsymbol{\theta})\|_2^2 \\ &= \frac{1}{N}\sum_{k=0}^{N-1}\left(y_d(k) - y(k;\boldsymbol{\theta})\right)^2. \end{aligned} \tag{21}$$

Partial differentiation of the evaluation function $J_{MR}(\boldsymbol{\theta})$ with respect to the parameter vector of the controller yields

$$\frac{\partial J_{MR}(\boldsymbol{\theta})}{\partial \boldsymbol{\theta}} = -\frac{2}{N}\sum_{k=0}^{N-1}\left(\frac{\partial y(k;\boldsymbol{\theta})}{\partial \boldsymbol{\theta}}\right)\left(y_d(k) - y(k;\boldsymbol{\theta})\right). \tag{22}$$

Then, the gradient of $y(i;\boldsymbol{\theta})$ is computed from (10) as follows:

$$\begin{aligned} \frac{\partial y(k;\boldsymbol{\theta})}{\partial \boldsymbol{\theta}} = \frac{1}{\bar{u}_0(0)}\Bigg\{ &\sum_{i=0}^{k-1}\bar{y}_0(k-i)\left[\left(r(i) - y(i;\boldsymbol{\theta})\right)\boldsymbol{C}_0^T(z)\right] \\ &- \sum_{i=0}^{k-1}\bar{y}_0(k-i)\left[\frac{\partial y(i;\boldsymbol{\theta})}{\partial \boldsymbol{\theta}}\boldsymbol{C}_0^T(z)\right]\boldsymbol{\theta} \\ &- \sum_{i=0}^{k-1}\frac{\partial y(i;\boldsymbol{\theta})}{\partial \boldsymbol{\theta}}\bar{u}_0(k-i)\Bigg\}. \end{aligned} \tag{23}$$

Since $y(0;\boldsymbol{\theta})$ takes a constant value (namely, the initial state), regardless of $\boldsymbol{\theta}$, (23) becomes

$$\frac{\partial y(0;\boldsymbol{\theta})}{\partial \boldsymbol{\theta}} = \mathbf{0}. \tag{24}$$

The gradient of $y(k;\boldsymbol{\theta})$ can, therefore, be computed sequentially from (23) and (24). Since $J_{MR}(\boldsymbol{\theta})$ is a polynomial with respect to $\boldsymbol{\theta}$, $J_{MR}(\boldsymbol{\theta})$ is minimized for $\boldsymbol{\theta}$ that satisfies

$$\frac{\partial J_{MR}(\boldsymbol{\theta})}{\partial \boldsymbol{\theta}} = \mathbf{0}. \tag{25}$$

One of the solutions of (25) can be obtained using Newton's method. For applying Newton's method, first, the Hessian matrix $\boldsymbol{H}(\boldsymbol{\theta})$ of $J_{MR}(\boldsymbol{\theta})$ must be found

$$\boldsymbol{H}(\boldsymbol{\theta}) = \frac{\partial}{\partial \boldsymbol{\theta}^T}\left(\frac{\partial J_{MR}(\boldsymbol{\theta})}{\partial \boldsymbol{\theta}}\right)$$

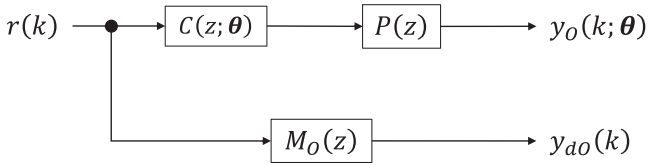

Fig. 3. Open-loop version of the model reference control problem.

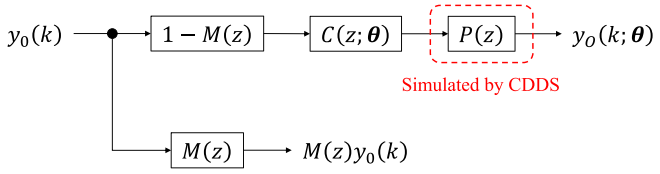

Fig. 4. Block diagram of the tuning process by the LS method in the CDDS framework.

$$= \frac{2}{N}\sum_{k=0}^{N-1}\left(\frac{\partial y\left(k;\boldsymbol{\theta}\right)}{\partial \boldsymbol{\theta}}\right)\left(\frac{\partial y\left(k;\boldsymbol{\theta}\right)}{\partial \boldsymbol{\theta}}\right)^{T} + \frac{2}{N}\sum_{k=0}^{N-1}\left(\frac{\partial^2 y\left(k;\boldsymbol{\theta}\right)}{\partial \boldsymbol{\theta}^T\partial \boldsymbol{\theta}}\right) y\left(k;\boldsymbol{\theta}\right). \tag{26}$$

Further differentiation of (23) yields

$$\frac{\partial^2 y\left(k;\boldsymbol{\theta}\right)}{\partial \boldsymbol{\theta}^T\partial \boldsymbol{\theta}} = -\frac{1}{\bar{u}_0(0)}\left\{\sum_{i=0}^{k-1}\bar{y}_0\left(k-i\right)\left[\frac{\partial y\left(i;\boldsymbol{\theta}\right)}{\partial \boldsymbol{\theta}}\boldsymbol{C}_0^T(z)\right]^T + \sum_{i=0}^{k-1}\bar{y}_0\left(k-i\right)\left[\frac{\partial^2 y\left(i;\boldsymbol{\theta}\right)}{\partial \boldsymbol{\theta}^T\partial \boldsymbol{\theta}}\boldsymbol{C}_0^T(z)\right]\boldsymbol{\theta} + \sum_{i=0}^{k-1}\frac{\partial^2 y\left(i;\boldsymbol{\theta}\right)}{\partial \boldsymbol{\theta}^T\partial \boldsymbol{\theta}}\bar{u}_0\left(k-i\right)\right\}. \tag{27}$$

Therefore, the updating equation of Newton's method will be

$$\boldsymbol{\theta}_{m+1} = \boldsymbol{\theta}_m - \boldsymbol{H}^{-1}\left(\boldsymbol{\theta}_m\right)\left(\frac{\partial J_{MR}\left(\boldsymbol{\theta}_m\right)}{\partial \boldsymbol{\theta}}\right). \tag{28}$$

One solution that satisfies (25) can be obtained by iteratively computing (28) using an initial solution $\boldsymbol{\theta}_0$. However, this solution may not necessarily yield the globally optimal solution of $J_{MR}(\boldsymbol{\theta})$.

D. Noniterative Approach

In this study, the iterative calculations that were performed by Newton's method (see the previous section) were performed in a single calculation. Consider the model reference control problem in an open-loop system, such as that shown in Fig. 3. The nominal model $M(z)$ in the closed-loop system changes in the open-loop system as follows:

$$M_O(z) := \frac{M(z)}{1-M(z)}. \tag{29}$$

The CDDS results of (10) also change as shown below:

$$y_O\left(k;\boldsymbol{\theta}\right) = \frac{1}{\bar{u}_0(0)}\left\{\sum_{i=0}^{k-1}\bar{y}_0\left(k-i\right)\left[r(i)\boldsymbol{C}_0^T(z)\right] - \sum_{i=0}^{k-1}\boldsymbol{y}_{O0}^T(i)\bar{u}_0\left(k-i\right)\right\}\boldsymbol{\theta} =: \boldsymbol{y}_{O0}^T(k)\boldsymbol{\theta}. \tag{30}$$

Therefore, the evaluation function for the model reference control problem in an open-loop system takes the following form:

$$J_O\left(\boldsymbol{\theta}\right) := \left\|y_{dO}(k) - y_O\left(k;\boldsymbol{\theta}\right)\right\|_2^2 = \frac{1}{N}\sum_{k=0}^{N-1}\left(y_{dO}(k) - y_O\left(k;\boldsymbol{\theta}\right)\right)^2 \tag{31}$$

where the gradient of $J_O(\boldsymbol{\theta})$ is as follows:

$$\frac{\partial J_O\left(\boldsymbol{\theta}\right)}{\partial \boldsymbol{\theta}} = -\frac{2}{N}\sum_{k=0}^{N-1}\left(\frac{\partial y_O\left(k;\boldsymbol{\theta}\right)}{\partial \boldsymbol{\theta}}\right)\left(y_{dO}(k) - y_O\left(k;\boldsymbol{\theta}\right)\right). \tag{32}$$

Unlike the iterative approach described in the previous section, the optimal parameter vector of the controller $\boldsymbol{\theta}^*$ that minimizes $J_O(\boldsymbol{\theta})$ can be calculated as

$$\frac{\partial J_O\left(\boldsymbol{\theta}^*\right)}{\partial \boldsymbol{\theta}} = \boldsymbol{0}$$

$$\boldsymbol{\theta}^* = \left(\sum_{k=0}^{N-1}\boldsymbol{y}_{O0}(k)\boldsymbol{y}_{O0}^T(k)\right)^{-1}\left(\sum_{k=0}^{N-1}\boldsymbol{y}_{O0}(k)y_{dO}(k)\right) \tag{33}$$

because $y_O(k;\boldsymbol{\theta})$ is a linear equation with respect to $\boldsymbol{\theta}$. However, the use of this equation may cause deviation of the CDDS operating point from the experimental data, further leading to the deterioration of the simulation accuracy. Furthermore, the controller cannot handle the case in which there is a minor loop feedback of the plant output. These problems can be solved as follows.

First, we construct $r(i)$ in a favorable form for simulation accuracy as there is no limitation on the reference signal $r(i)$ when calculating $\boldsymbol{y}_{O0}(k)$. Here, $r(k)$ is written as

$$r(i) = \left(1 - M(z)\right)y_0(i) \tag{34}$$

implying that the CDDS will operate near $M(z)y_0(i)$. The optimal parameter vector of the controller $\boldsymbol{\theta}^*$ will be

$$\boldsymbol{\theta}^* = \left(\sum_{k=0}^{N-1}\boldsymbol{y}_{O0}(k)\boldsymbol{y}_{O0}^T(k)\right)^{-1}\left(\sum_{k=0}^{N-1}\boldsymbol{y}_{O0}(k)M(z)y_0(k)\right). \tag{35}$$

Under the assumption of ideal tuning is performed ideally, the minor loop feedback terms of the controller (e.g., the current feedback) are set as $M(z)y_0(i)$. The final block diagram is as shown in Fig. 4. The parameter vector of the controller $\boldsymbol{\theta}$ that is optimized via (35) is the solution obtained by the least-squares (LS) method by only a single calculation. Table I provides a

TABLE I
SUMMARY OF THE CONTROLLER DESIGN METHODS USED WITH THE PROPOSED CDDS METHOD

Approach	Whether applicable to other data-driven simulations?	Optimization method
Direct	Partially yes	Optimization solvers
Iterative	No	Gradient method
Noniterative	No	Least-squares method

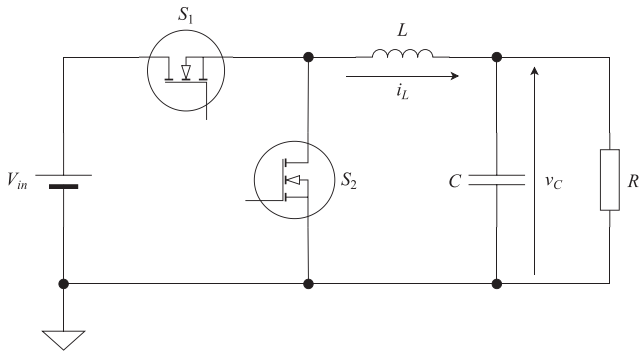

Fig. 5. Schematic of the buck converter. V_{in}, L, C, and R are the input voltage, inductance, capacitance, and load resistance, respectively.

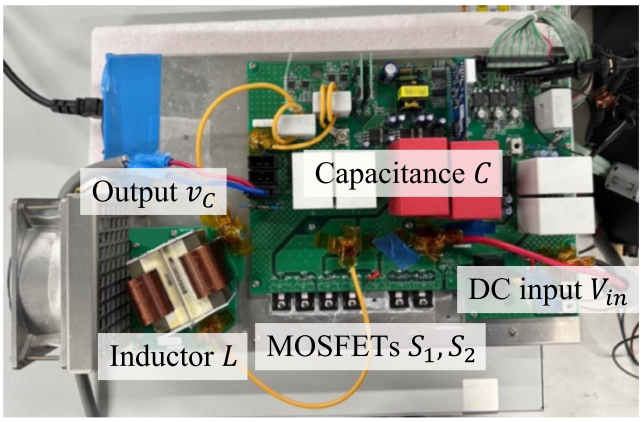

Fig. 6. Photograph of the experimental system.

summary of the controller design methodology. Note that the iterative and noniterative approaches are variants of the simulation equations obtained by CDDS, and these approaches cannot be directly applied to other data-driven simulation methods.

IV. APPLICATION EXAMPLE

A. Plant Specifications

The performance of the proposed CDDS method was assessed by applying the CDDS method to the buck converter, as shown in Figs. 5 and 6. The specifications of the buck converter are summarized in Table II. The controller is a digital proportional–integral (PI) controller with an inductor current feedback for voltage regulation, as shown in Fig. 7. Here, V_r, v_C, i_L, and T are the reference voltage, output voltage, inductor current, and sampling period, respectively. Further, K_P, K_I, and K_L are the P gain, I gain, and inductor current feedback gain, respectively,

TABLE II
SPECIFICATIONS OF THE BUCK CONVERTER

Parameter	Value
Input voltage V_{in}	380 V
Output voltage v_C	0 V to 300 V
Inductance L	135 μH
Capacitance C	100 μF
Load resistance R	24.7 Ω to 365 kΩ(no load)
Sampling period T	10 μs
Switching frequency f_s	100 kHz

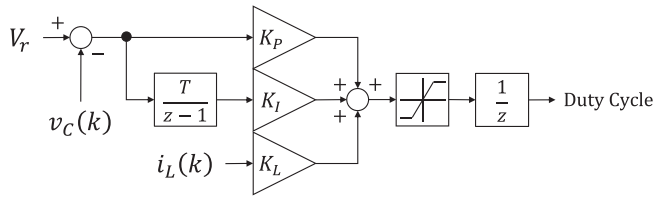

Fig. 7. Digital PI controller with an inductor current feedback.

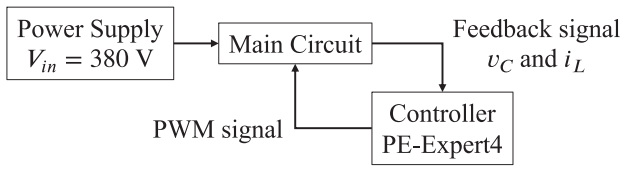

Fig. 8. Overview of the experimental system.

which are the control parameters that need to be tuned. The output of this controller has a saturation characteristic that is equivalent to the feasible duty cycle of pulsewidth modulation (PWM), as well as a one-sample delay due to digital processing. An overview of the system used in the experiment is shown in Fig. 8.

B. Experimental Conditions

This section presents a comparison of the results obtained by the CDDS method with the results obtained by three conventional methods. The virtual time-response-based iterative gain evaluation and redesign (V-Tiger) method was selected as a data-driven simulation approach, and the VRFT, and NCbT methods were selected as data-driven control methods. The root-mean-square error (RMSE) between the actual and calculated responses was used to evaluate the performances of the V-Tiger and CDDS methods, and the RMSE between the actual and desired responses was used to evaluate the performances of the VRFT, NCbT, and CDDS methods.

The control parameters that were used to collect the experimental data were determined by the pole assignment method [16]. Experimental data were obtained by separating the five operating points (OP1–OP5) in increments of 50 V over the range of 50–300 V using the control parameters determined by the pole assignment method. For example, the experimental data in OP1 represent the case that a reference value with a 50 V amplitude is obtained from a state of convergence to 50 V. The experimental data for each operating point with offset

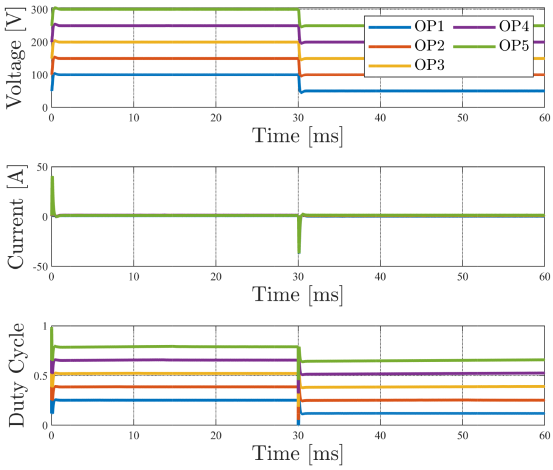

Fig. 9. Collected experimental data. The inductor currents overlap at each operating point.

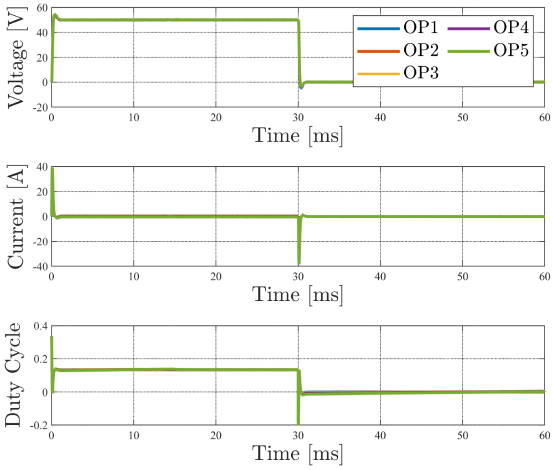

Fig. 10. Experimental data with offset cancelation.

cancelation by (8) and (9) are shown in Figs. 9 and 10. The absolute values of the eigenvalues of matrix $\boldsymbol{A}$ in (16), which are related to the convergence of the estimation error of CDDS, are shown in Fig. 11. The results confirm that there are no unstable poles that adversely affect the estimation.

The following fourth-order system was used as the nominal model to tune the controller:

$$M(z) = \left. \frac{(4\omega_0)^4}{(s+4\omega_0)^4} \right|_{s=\frac{2(z-1)}{T(z+1)}} \tag{36}$$

where ω_0 is the resonance frequency ($\omega_0 = 1/\sqrt{LC}$). The model reference control problem (21) was optimized via the Nelder–Mead method for CDDS-based tuning. Specifically, the optimization was performed via simulation with CDDS according to the following equation:

$$u_c(k+1) = K_L i_L(k) + \left(K_P + \frac{TK_I}{z-1}\right)(V_r - v_C(k)) \tag{37}$$

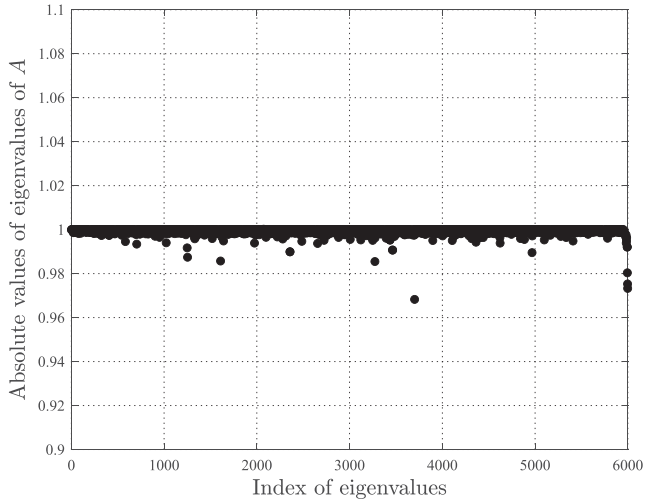

Fig. 11. Absolute values of eigenvalues of matrix $\boldsymbol{A}$ in (16).

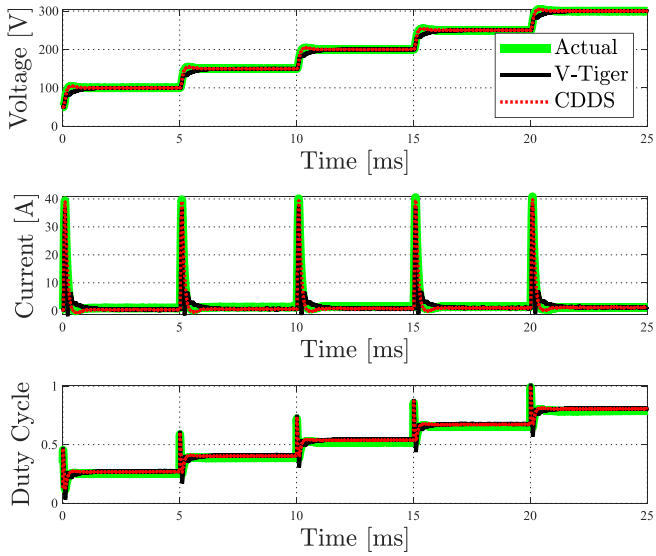

Fig. 12. Comparison of the actual responses and data-driven simulation results of the V-Tiger and CDDS methods using the OP3 data (150–200 V).

$$u(k) = \begin{cases} 1 & \text{if } u_c(k) > 1 \\ 0 & \text{if } u_c(k) < 0 \\ u_c(k) & \text{otherwise} \end{cases} \tag{38}$$

where $u_c(k)$ is the input calculated by the controller and $u(k)$ is the actual input signal to the plant, obtained by considering saturation. CDDS was performed using $u(k)$ for output voltage $v_C(k)$ and inductor current $i_L(k)$.

C. Data-Driven Simulation Results

A comparison of data-driven simulations via the V-Tiger and CDDS methods using the OP3 data is shown in Fig. 12. Table III provides a comparison of the corresponding RMSEs between the actual and calculated responses at all operating points (OP1–OP5). The estimation error

TABLE III
COMPARISON OF THE RMSES BETWEEN THE ACTUAL VALUES AND THE CALCULATED V-TIGER AND CDDS RESPONSES

Data	Voltage [V]		Current [A]		Duty Cycle	
	CDDS	V-Tiger	CDDS	V-Tiger	CDDS	V-Tiger
OP1	0.286	4.87	0.579	2.54	0.0148	0.0182
OP2	0.250	4.86	0.455	2.48	0.0103	0.0149
OP3	0.241	4.88	0.595	2.50	0.0164	0.0212
OP4	0.247	4.87	1.35	2.75	0.0126	0.0167
OP5	0.317	4.89	2.67	3.62	0.0106	0.0165
Average	0.268	4.87	1.13	2.78	0.0129	0.0175

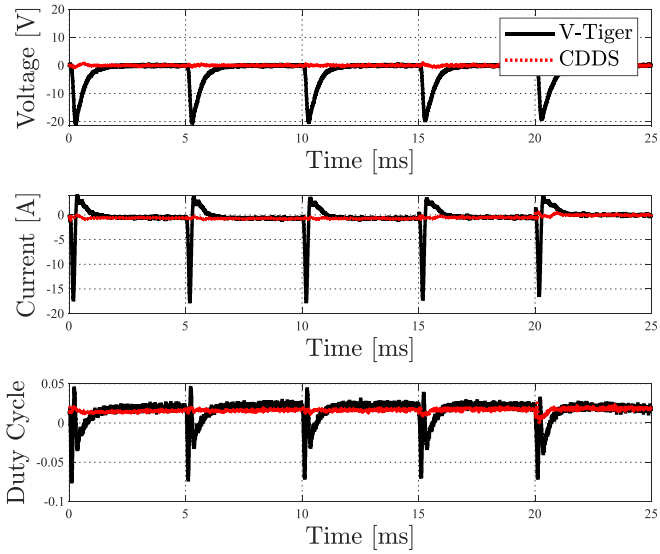

Fig. 13. Comparison of the estimation errors of the V-Tiger and CDDS methods using the OP3 data (150–200 V).

TABLE IV
COMPARISON OF THE RMSES BETWEEN THE DESIRED RESPONSE AND THE ACTUAL RESPONSES OF THE VRFT, NCBT, AND CDDS APPROACHES

Data	CDDS [V]	VRFT [V]	NCbT [V]
OP1	0.192	0.767	0.491
OP2	0.178	0.597	0.612
OP3	0.211	0.609	0.629
OP4	0.256	0.655	0.675
OP5	0.357	0.744	0.759
Average	0.239	0.675	0.633

using the OP3 data is shown in Fig. 13. The proposed CDDS method yielded a smaller RMSE than the conventional V-Tiger method at all operating points, highlighting that the CDDS method provides more accurate data-driven simulations.

D. Tuning Results

The tuning results obtained by the VRFT, NCbT, and CDDS methods using the OP3 data are shown in Fig. 14. Table IV presents a comparison of the corresponding RMSEs between the desired and actual responses at all operating points. The tuning error using the OP3 data is shown in Fig. 15. The RMSE of the proposed CDDS method was much smaller than the RMSEs of the conventional VRFT and

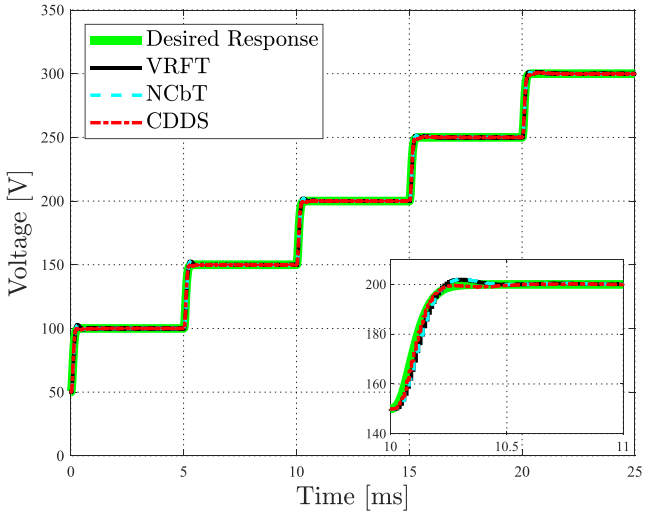

Fig. 14. Comparison of the tuning results obtained by the VRFT, NCbT, and CDDS methods using the OP3 data (150–200 V). A magnified view of the OP3 response is provided in the lower right.

TABLE V
COMPARISON OF CDDS WITH CONVENTIONAL DATA-DRIVEN SIMULATION METHODS

	CDDS	Subspace [18], [19]	V-Tiger [22]
Underlying theory	Transfer function	State-space model	Transfer function
Constraints on linearity of the controller	No	No	Yes
Computational cost	Low	High	Medium

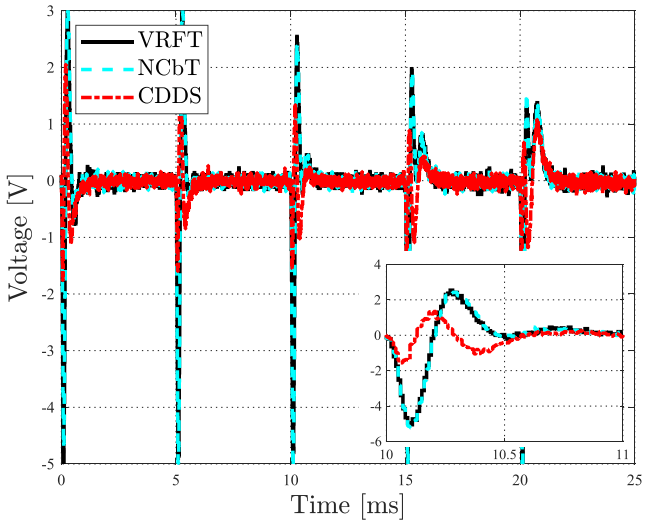

Fig. 15. Comparison of the tuning errors via the VRFT, NCbT, and CDDS methods using OP3 data (150–200 V). A magnified view of the OP3 tuning error is provided in the inset in the lower right.

NCbT methods at all operating points. This result highlights that the CDDS method effectively computes control parameters so that the response obtained is close to the desired response.

V. Conclusion

This article described a new data-driven simulation method, namely, the CDDS method and a CDDS-based controller design method. Unlike conventional methods, the CDDS method could explicitly consider the nonlinearity of controllers, thereby provided more flexibility in designing controllers. This was because the CDDS method only focused on the input–output relationship of the plant and did not impose any constraints on the characteristics of the controller. Therefore, the obtained controller was less conservative than that obtained by conventional methods, such as robust control. In addition, from Table V, we saw that the conventional method had the problems of huge computational cost which arose from the need for inverse matrix calculation and the nonlinearity of the controller. The CDDS method solved these problems.

The experimental results obtained using a buck converter demonstrated that the CDDS method could reduce the estimation errors by up to 95.0% compared with the V-Tiger method. The CDDS method could also reduce the tuning error by more than 52.0% compared with the VRFT and NCbT methods. These results meant that the CDDS method was more accurate than the conventional V-Tiger method in terms of data-driven simulation and provided tuning results that were closer to the desired response than the conventional VRFT and NCbT methods in terms of data-driven control.

The advantage of CDDS in converter applications was that the controller could be optimized at the time of shipment, even if the parameters of the circuit components varied from their nominal values. Furthermore, it was possible to tune the controller on site during maintenance.

Appendix

A. Detailed Algorithm for Iterative Approach

The controller design with the iterative approach is obtained by the following steps:

1) Collect experimental data (input $\bar{u}_0(k)$ and output $\bar{y}_0(k)$ data) for $0 \leq k \leq N-1$ for the system to be simulated.
2) Determine the initial control parameter $\boldsymbol{\theta}_0$.
3) Using (23) and (27), compute the gradient of the evaluation function and the Hessian matrix from (22) and (26), respectively.
4) Update the parameter $\boldsymbol{\theta}_m$ to $\boldsymbol{\theta}_{m+1}$ according to the update formula (28). If the update range is less than the threshold value, repeat from step 3).

B. Detailed Algorithm for Noniterative Approach

The controller design with the noniterative approach involves the following steps:

1) Collect input $\bar{u}_0(k)$ and output $\bar{y}_0(k)$ data for the system to be simulated. These data are collected from experiments for $0 \leq k \leq N-1$.
2) Determine the nominal model $M(z)$.
3) Calculate $\boldsymbol{y}_{O0}(k)$ from (30).
4) Calculate the optimal parameter vector of the controller $\boldsymbol{\theta}^*$ by (35).

References

[1] K. Prag, M. Woolway, and T. Celik, "Toward data-driven optimal control: A systematic review of the landscape," *IEEE Access*, vol. 10, pp. 32 190–32 212, 2022.

[2] H. Hjalmarsson, M. Gevers, S. Gunnarsson, and O. Lequin, "Iterative feedback tuning: Theory and applications," *IEEE Control Syst. Mag.*, vol. 18, no. 4, pp. 26–41, Aug. 1998.

[3] A. Karimi, L. Mišković, and D. Bonvin, "Convergence analysis of an iterative correlation-based controller tuning method," *IFAC Proc. Volumes*, vol. 35, no. 1, pp. 413–418, 2002.

[4] M. Campi, A. Lecchini, and S. Savaresi, "Virtual reference feedback tuning: A direct method for the design of feedback controllers," *Automatica*, vol. 38, no. 8, pp. 1337–1346, 2002.

[5] O. Kaneko, "Data-driven controller tuning: FRIT approach," *IFAC Proc. Volumes*, vol. 46, no. 11, pp. 326–336, 2013.

[6] A. Karimi, K. v. Heusden, and D. Bonvin, "Non-iterative data-driven controller tuning using the correlation approach," in *Proc. Eur. Control Conf.*, 2007, pp. 5189–5195.

[7] P. Yan, D. Liu, D. Wang, and H. Ma, "Data-driven controller design for general MIMO nonlinear systems via virtual reference feedback tuning and neural networks," *Neurocomputing*, vol. 171, pp. 815–825, 2016.

[8] S. Bradtke, B. Ydstie, and A. Barto, "Adaptive linear quadratic control using policy iteration," in *Proc. Amer. Control Conf.*, 1994, pp. 3475–3479.

[9] Z. Hou, C. Han, and W. Huang, "The model-free learning adaptive control of a class of MISO nonlinear discrete-time systems," *IFAC Proc. Volumes*, vol. 31, no. 25, pp. 227–232, 1998.

[10] S. Arimoto, S. Kawamura, and F. Miyazaki, "Bettering operation of dynamic systems by learning: A new control theory for servomechanism or mechatronics systems," in *Proc. IEEE 23rd Conf. Decis. Control*, 1984, pp. 1064–1069.

[11] S. Schaal and C. Atkeson, "Robot juggling: Implementation of memory-based learning," *IEEE Control Syst. Mag.*, vol. 14, no. 1, pp. 57–71, Jan. 1994.

[12] C. L. Remes, G. R. G. d. Silva, A. Treviso, M. A. Coelho, and L. Campestrini, "Data-driven approach for current control in DC-DC boost converters," *IFAC-PapersOnLine*, vol. 52, no. 1, pp. 190–195, 2019.

[13] C. L. Remes, R. B. Gomes, J. V. Flores, F. B. Líbano, and L. Campestrini, "Virtual reference feedback tuning applied to DC–DC converters," *IEEE Trans. Ind. Electron.*, vol. 68, no. 1, pp. 544–552, Jan. 2021.

[14] Y. Gohda, S. Masuda, and Y. Matsui, "A direct PID gain tuning based on FRIT method using optimal filter in the frequency domain," *IFAC Proc. Volumes*, vol. 46, no. 11, pp. 349–354, 2013.

[15] Y. Kansha, Y. Hashimoto, and M.-S. Chiu, "New results on VRFT design of PID controller," *Chem. Eng. Res. Des.*, vol. 86, no. 8, pp. 925–931, 2008.

[16] N. Kameya, Y. Fujimoto, Y. Hosoyamada, and T. Suenaga, "VRFT for current-mode buck converter with anti-windup compensation," in *Proc. IEEE Energy Convers. Congr. Expo.*, 2022, pp. 1–7.

[17] K. Åström and T. Hägglund, "The future of PID control," *Control Eng. Pract.*, vol. 9, no. 11, pp. 1163–1175, 2001.

[18] I. Markovsky, J. C. Willems, P. Rapisarda, and B. L. D. Moor, "Data driven simulation with applications to system identification," *IFAC Proc. Volumes*, vol. 38, no. 1, pp. 970–975, 2005.

[19] I. Markovsky and P. Rapisarda, "Data-driven simulation and control," *Int. J. Control*, vol. 81, no. 12, pp. 1946–1959, 2008.

[20] O. Kaneko and T. Nakamura, "Data-driven prediction of 2DOF control systems with updated feedforward controller," in *Proc. IEEE 56th Annu. Conf. Soc. Instrum. Control Engineers Jpn.*, 2017, pp. 259–262.

[21] R. Hoogendijk, M. v. d. Molengraft, A. d. Hamer, G. Angelis, and M. Steinbuch, "Computation of transfer function data from frequency response data with application to data-based root-locus," *Control Eng. Pract.*, vol. 37, pp. 20–31, 2015.

[22] M. Kosaka, A. Kosaka, and M. Kosaka, "Virtual time-response based iterative gain evaluation and redesign," *IFAC-PapersOnLine*, vol. 53, no. 2, pp. 3946–3952, 2020.

[23] J. C. Lagarias, J. A. Reeds, M. H. Wright, and P. E. Wright, "Convergence properties of the Nelder–Mead simplex method in low dimensions," *SIAM J. Optim.*, vol. 9, no. 1, pp. 112–147, 1998.

Naoki Kameya was born in Kanagawa Prefecture, Japan. He received the B.E. degree in electrical and computer engineering in 2022 from Yokohama National University, Yokohama, Japan, where he is currently working toward the M.E. degree in electrical and computer engineering.

His research interests include data-driven control of dc-dc converters.

Yasutaka Fujimoto (Senior Member, IEEE) was born in Kanagawa Prefecture, Japan. He received the B.E., M.E., and Ph.D. degrees in electrical and computer engineering from Yokohama National University, Yokohama, Japan, in 1993, 1995, and 1998, respectively.

In 1998, he was with the Department of Electrical Engineering, Keio University, Yokohama, Japan. Since 1999, he has been with the Department of Electrical and Computer Engineering, Yokohama National University, Yokohama, where he is currently a Professor. His research interests include actuators, robotics, manufacturing automation, and motion control.

Dr. Fujimoto is an Associate Editor for the IEEE TRANSACTIONS ON INDUSTRIAL ELECTRONICS and *IEEJ Journal of Industry Applications*.

Yu Hosoyamada (Member, IEEE) received the B.E., M.E., and Ph.D. degrees in electrical and computer engineering from Yokohama National University, Yokohama, Japan, in 2013, 2015, and 2021, respectively.

Since 2015, he has been with Kyosan Electric Manufacturing Company Ltd., Yokohama, Japan. His research interests include power electronics and RF technology.

Toyoaki Suenaga received the B.E. degree in faculty of engineering from Kyushu Institute of Technology, Fukuoka, Japan, in 1989.

He joined Kyosan Electric Mfg. Company, Ltd., Yokohama, Japan in 1989. His research interests are power electronics in general and RF, High Voltage dc technology.